Simulating Two-Fluid MHD Dynamos
And
A Novel Paradigm for Geodesic Mesh MHD

By

Dinshaw Balsara, Sudip Garain (UND), Alex Lazarian, Siyao Xu (UWisc), Vladimir Florinski (UAH)

Turbulent Two-Fluid MHD Dynamos

Dynamo action Amplifies strength of Magnetic field in a plasma and Increases the coherence length of the magnetic field.

Small-scale dynamo has fastest growth; so we focus on that.

Most astrophysical magnetic fields undergo dynamo action in partially ionized plasmas. Therefore, two-fluid, partially ionized plasmas constitute the focus on this study. Never studied before.

Analytical theory for turbulent, small-scale dynamos in partially ionized plasmas makes two very important predictions (Xu & Lazarian 2016, 2017) – unique to partially ionized plasmas.

We have verified those predictions via simulations.

Applications to molecular clouds and early universe.

Single Fluid Small-scale Dynamos V/S Two-Fluid Small-scale Dynamos:-

In both, the turbulent motions result in a stretch-twist-fold process which increases the field strength.

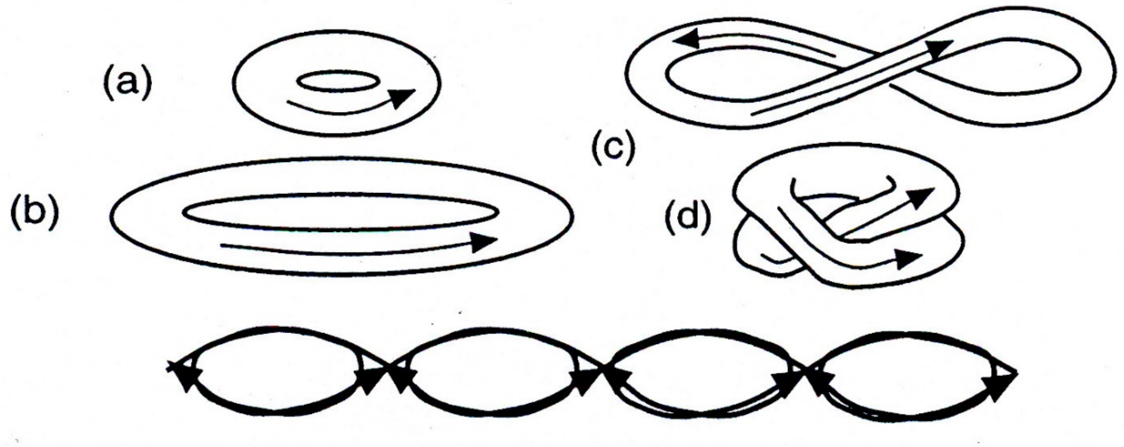

(e)

Magnetic energy builds up fastest on the smallest scales. However, in order for the small scale magnetic fields to not quench the dynamo, there has also to be a small scale dissipation.

For single fluid MHD (highly ionized plasma) turbulent diffusion provides small scale dissipation.

For two-fluid MHD (partially ionized plasma) ion-neutral friction provides small scale dissipation. For very low ionization, the ions collide so infrequently with the neutrals that the KE of the neutrals is very inefficiently converted into magnetic energy. Small scale equipartition never reached.

Governing Equations for Partially-Ionized Fluids

$$\rho_i\left(\frac{\partial \mathbf{v}_i}{\partial t}+(\mathbf{v}_i\cdot\nabla)\mathbf{v}_i\right)+\nabla P_i+\rho_i\nabla\Phi+\frac{1}{4\pi}\mathbf{B}\times(\nabla\times\mathbf{B})=-\alpha\rho_n\rho_i(\mathbf{v}_i-\mathbf{v}_n)$$

$$\rho_n\left(\frac{\partial \mathbf{v}_n}{\partial t}+(\mathbf{v}_n\cdot\nabla)\mathbf{v}_n\right)+\nabla P_n+\rho_n\nabla\Phi=-\alpha\rho_n\rho_i(\mathbf{v}_n-\mathbf{v}_i)$$

V.V. Imp.

$L_{AD}=\mathrm{V}_A/\alpha\rho_i$ ~ 0.01 -- 0.05 pc for fiducial parameters

Trends: $(L_{AD}\uparrow$ as $\rho_i\downarrow)$ and $(L_{AD}\uparrow$ as $\mathbf{B}\uparrow)$

(protostellar cores also form on this length scale $\Rightarrow$ it is v. important)

Recall: ξ~10^{-6} to 10^{-8}

In the past: $\mathrm{V}_{A-ion}=B/\sqrt{4\pi\rho_i}$ was deemed too large for practical computations -- The heavy ion approximation (HIA) was the compromise. HIA was found to discard essential physics -- HIA not used here.

First Prediction from theory:-

Magnetic field would initially undergo exponential growth with time.

Once L_{AD} reaches $L_{driving}$, it undergoes linear growth with increasing time.

Well-resolved 1024^3 zone, and upwards , simulations were needed o prove this.

BW is/was unique machine for the task.

Computations v.v. time-consuming!

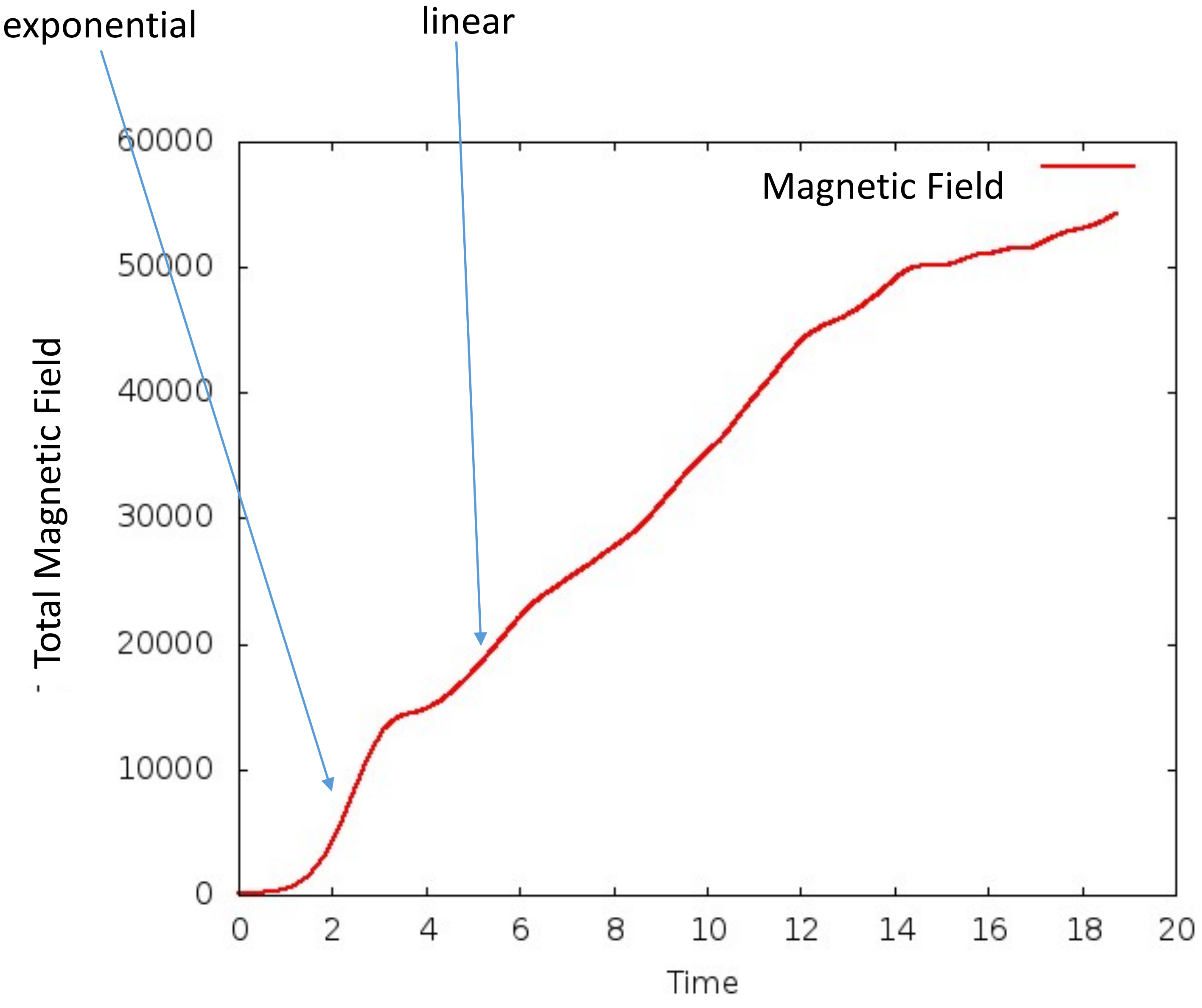

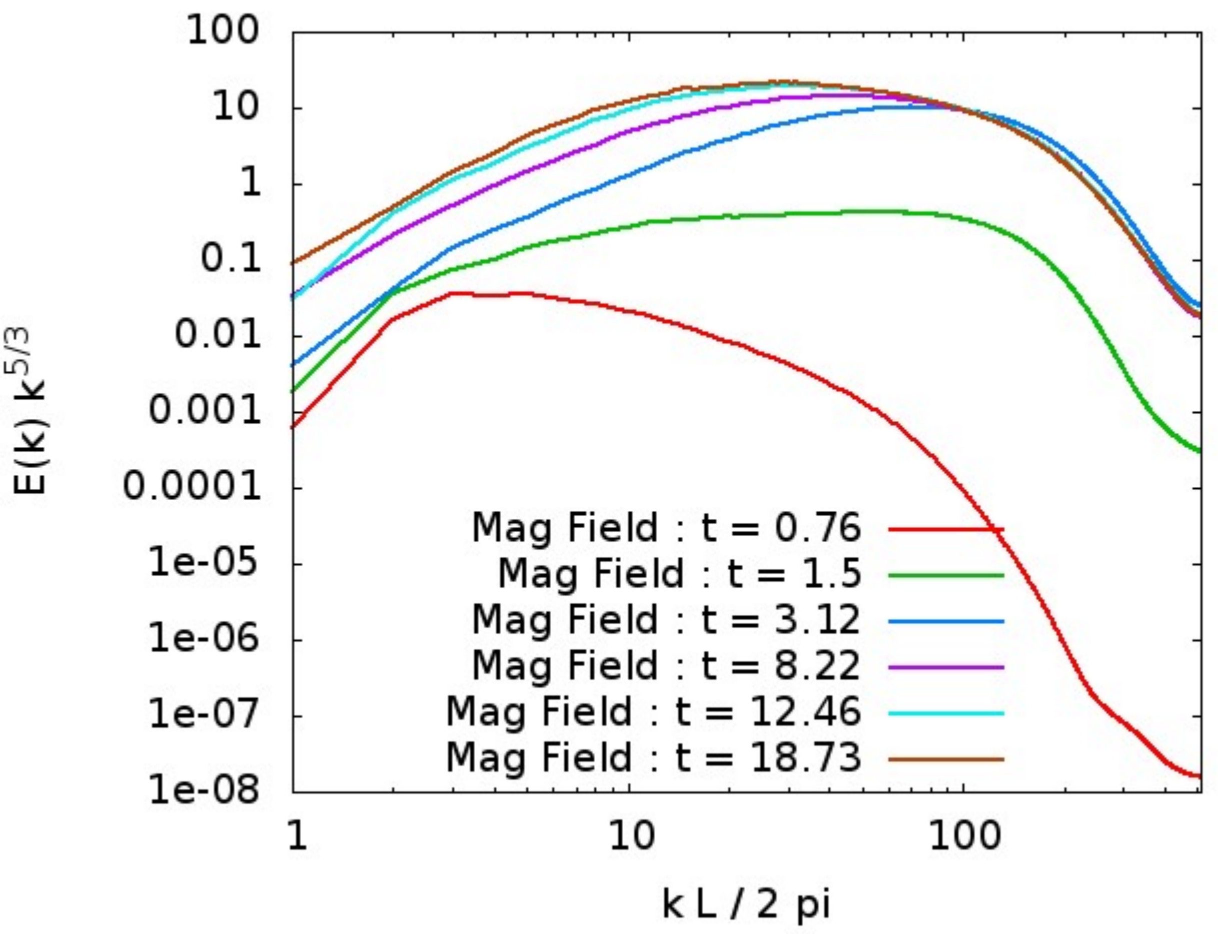

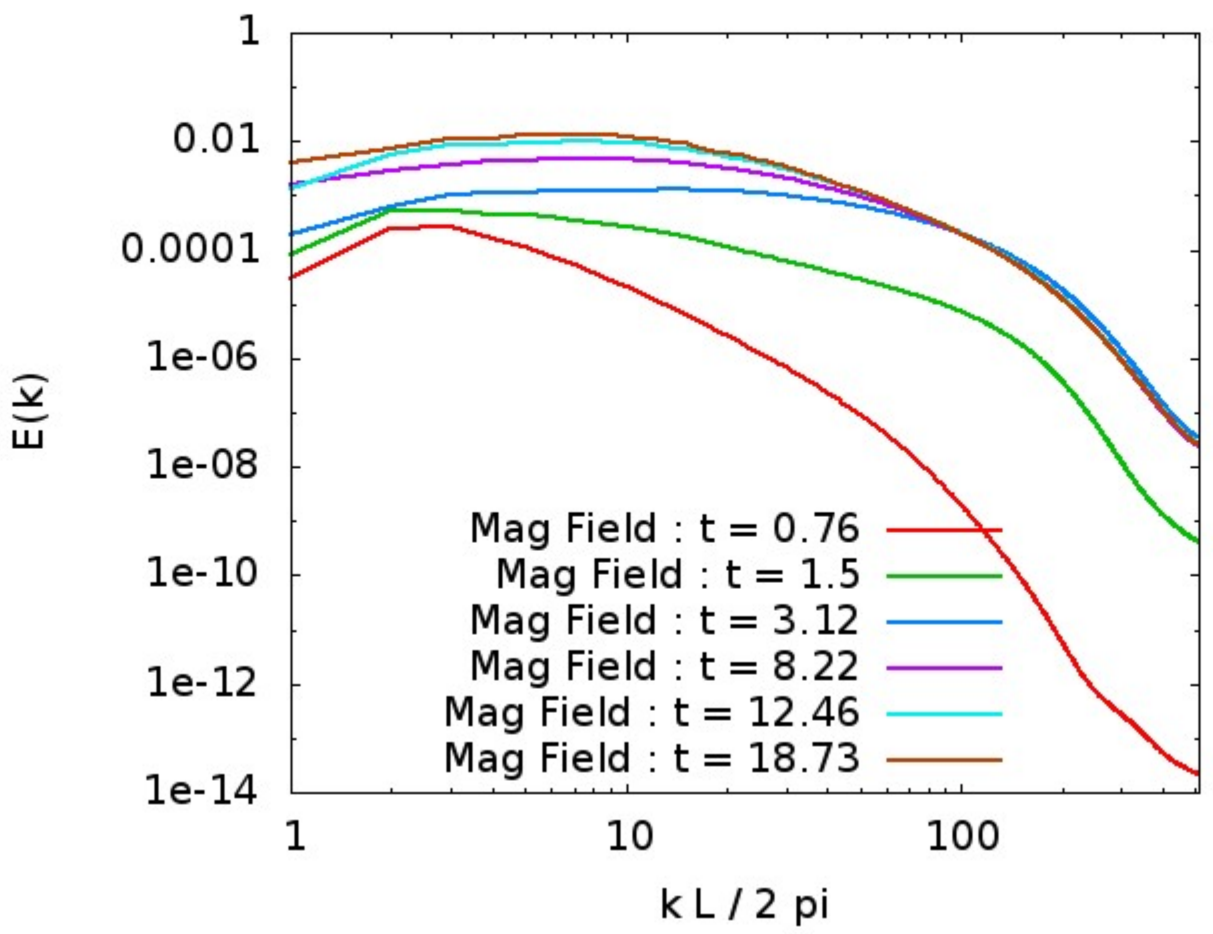

Second Prediction from Theory:-

The peak in the magnetic energy spectrum migrates initially to small scales. With increasing time, that peak migrates back to larger scales.

Geodesic Mesh MHD

I) "On Being Round"

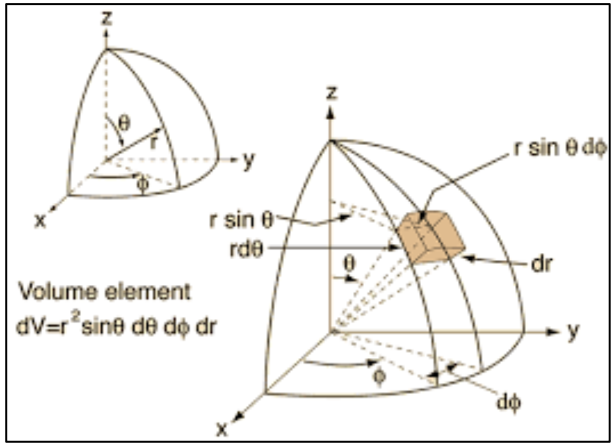

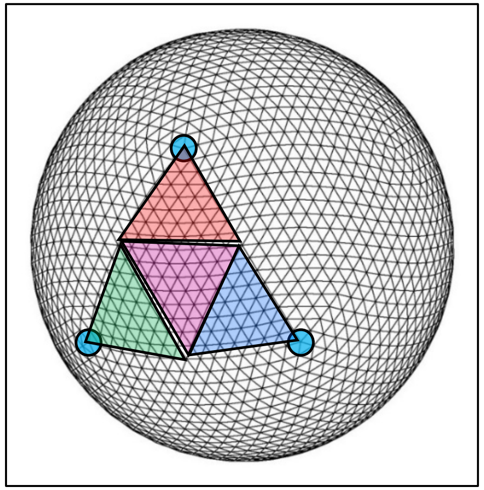

Problem: Several Astrophysical systems are spherical;
Codes for simulating them have been logically Cartesian. (r-θ-ϕ coordinates)
Timestep and accuracy problems at poles!

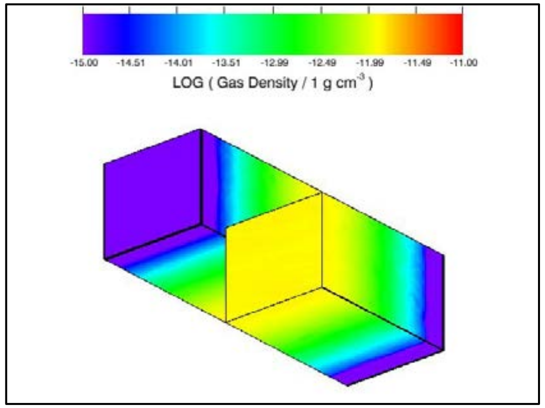

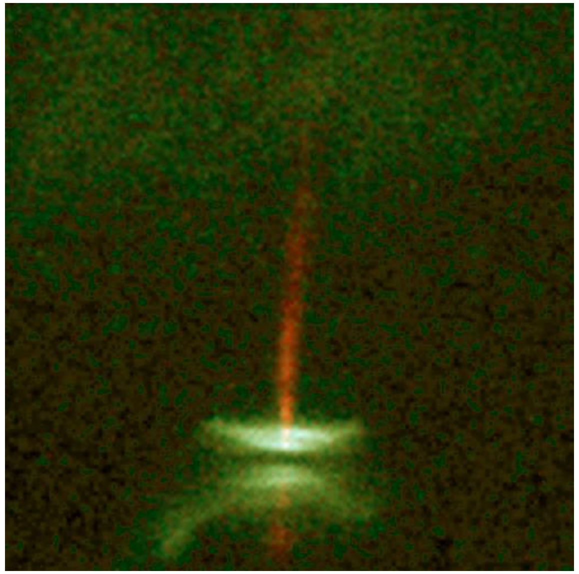

Example systems:-
Accretion Disks and MRI – Done in Shearing Sheet boxes

Jets propagating in pressure gradients around Galaxies

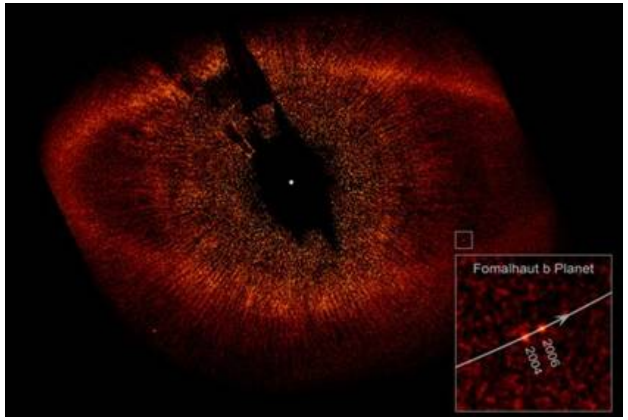

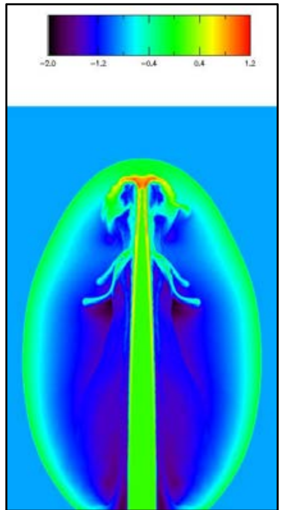

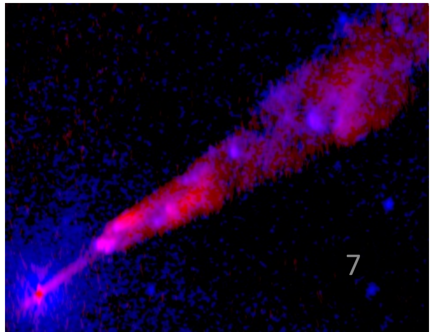

Star and Planet Formation

Heliosphere

Magnetospheres of planets

Convection in the Sun

Convection in AGB Stars

Supernovae

Possible uses in Galaxy formation

Possible uses in NS-NS collisions

Atmospheres of Proto-planets

Global Weather

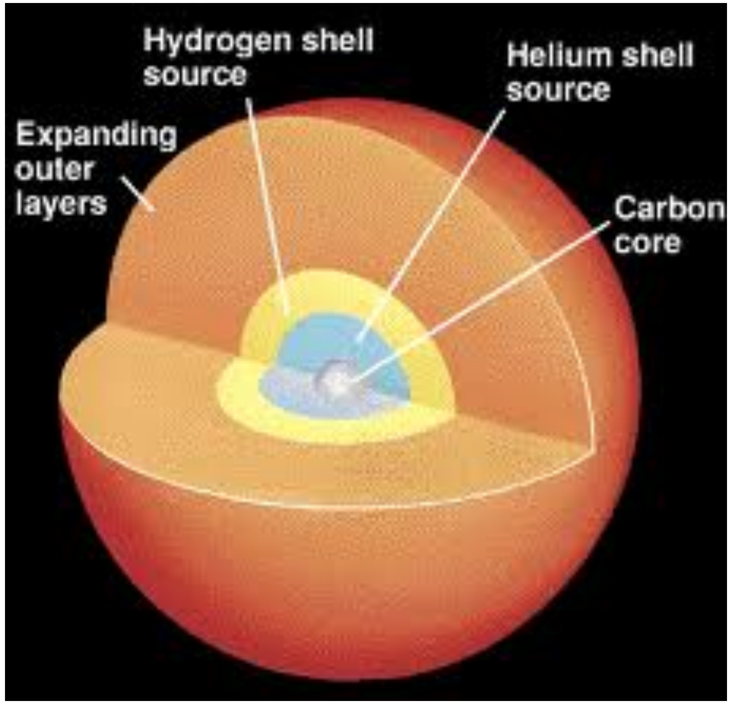

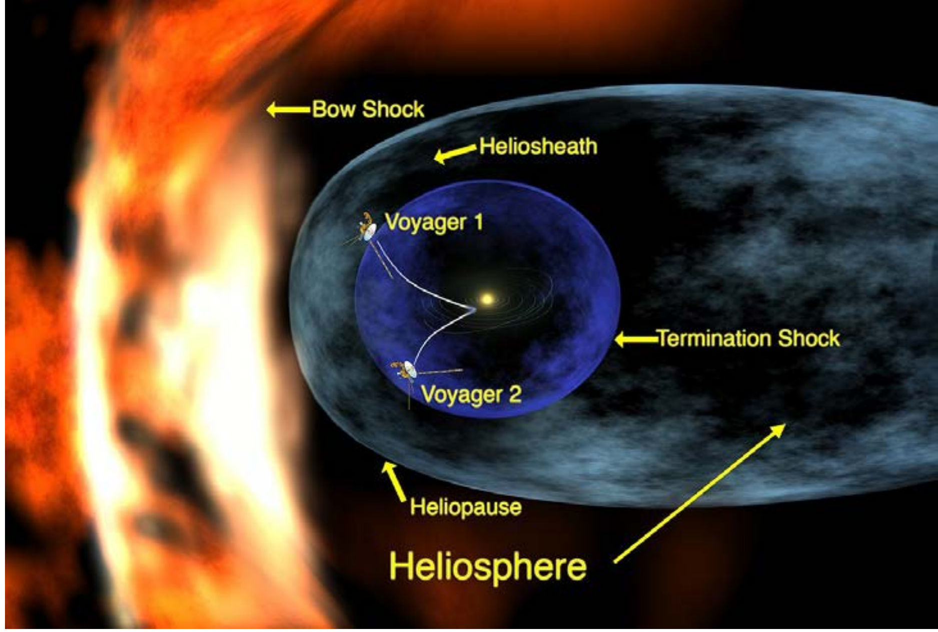

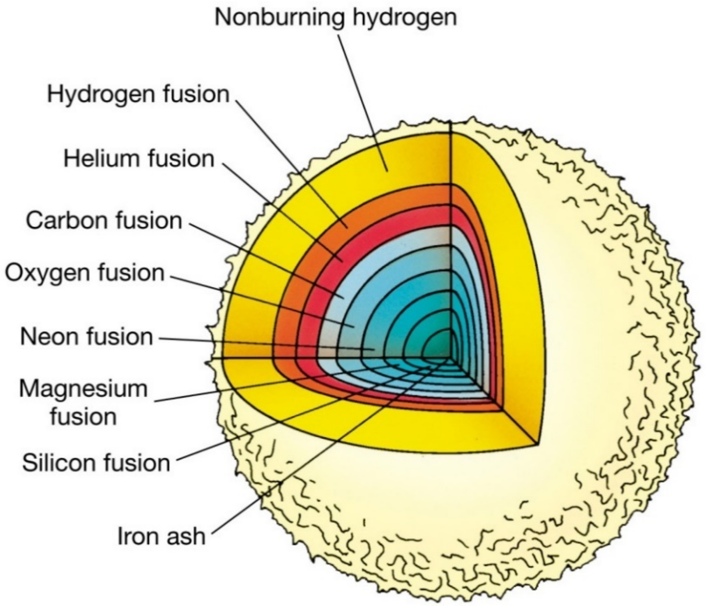

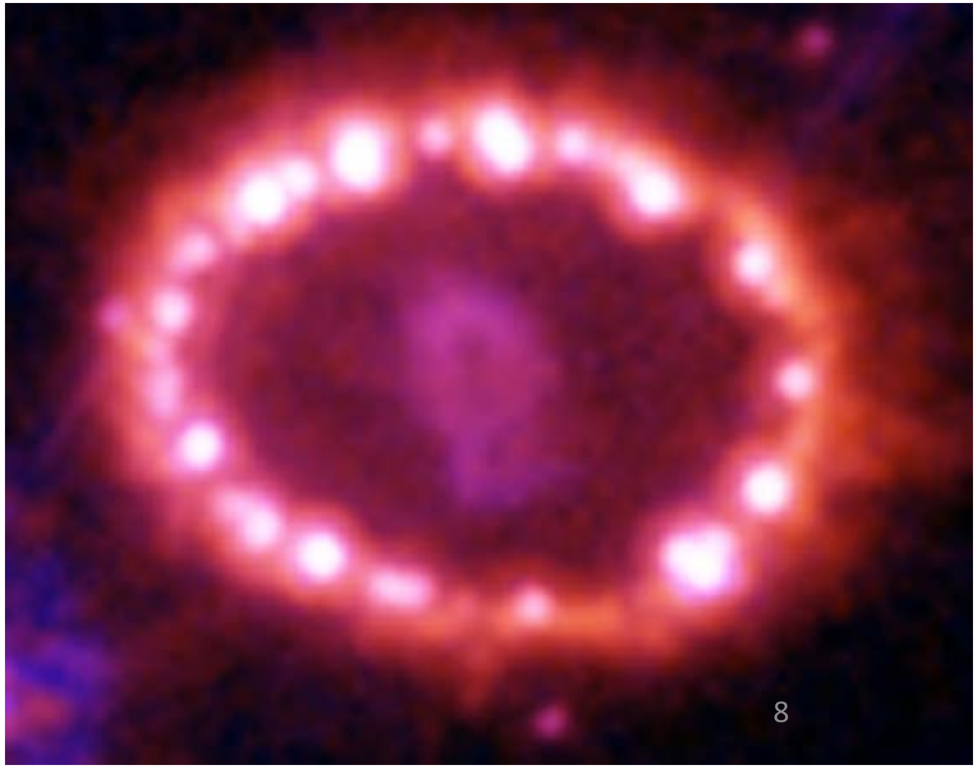

Because of need for turbulence modeling, we need to learn how to do higher order MHD optimally in spherical systems!

II) Geodesic Meshes and their Advantages – The Challenge of Meshing the Sphere:-

The Computer Simulation of all such systems is hampered by the fact that spherical coordinate systems result in vanishingly **small timesteps**, and a **loss of accuracy close to the poles**. This is a coordinate singularity and should be removable.

For General Relativistic systems, we want to **go as close to the physical singularity** at event horizon without blow-up.

The Underlying Mesh should be free of these defects. It should give us the **maximum possible angular isotropy**.

Icosahedron

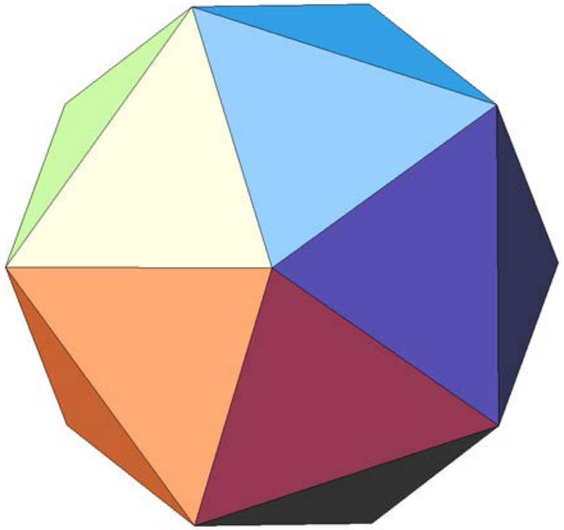

Spherical Icosahedron
Level 0 sector

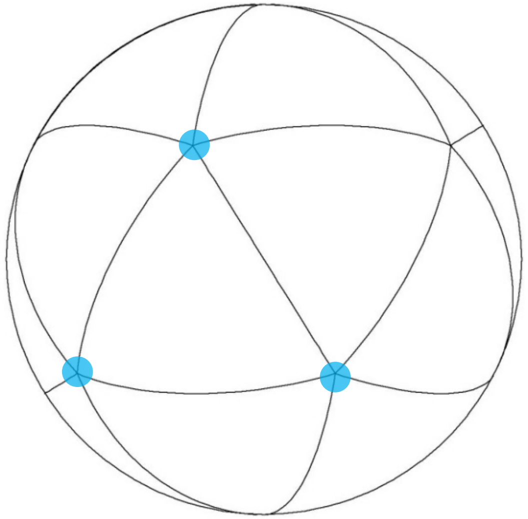

Level 1 sector division

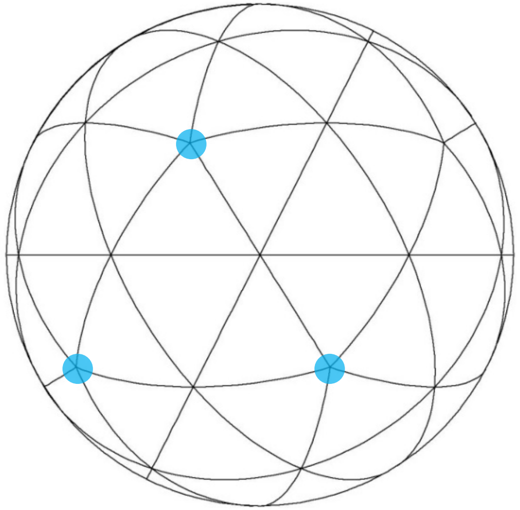

Level 4 zoning within each level 1 sector.

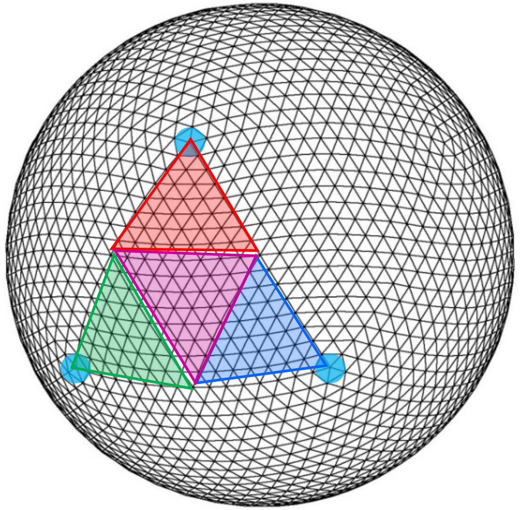

Extrude the mesh in the radial direction to get a 3D mesh:-
(Done here for a level 1 sector from the previous page.)

Resulting zones have a shape called a fustrum.

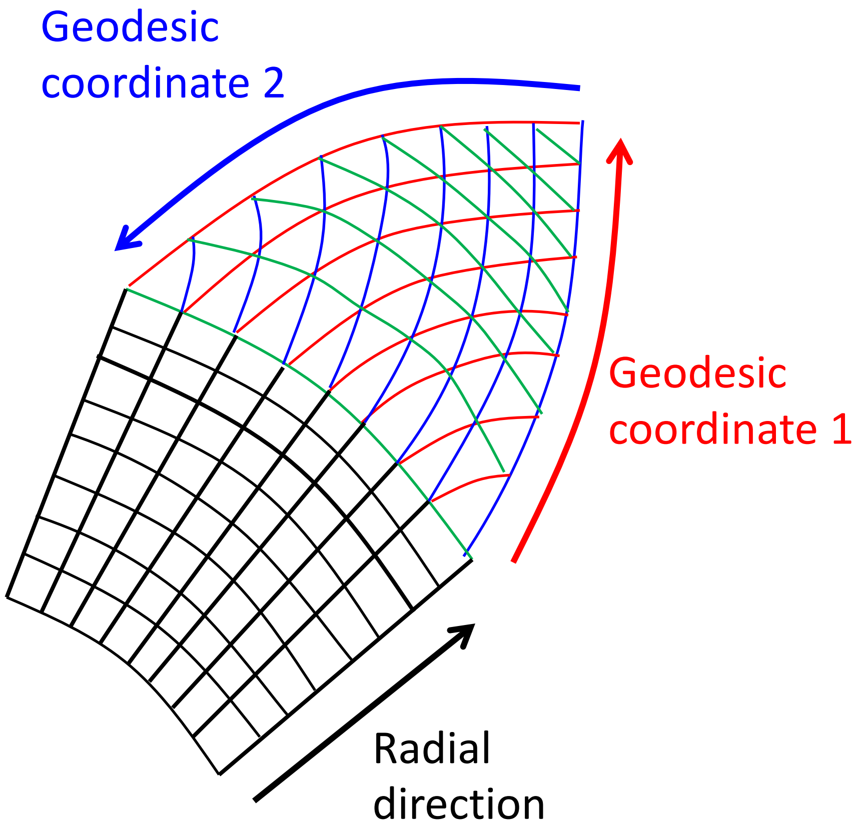

III) High Accuracy Divergence-Free MHD on Geodesic Meshes – Algorithmic Issues

Built on the following four easy steps:-

i) High order WENO Reconstruction on Unstructured Meshes.

ii) Divergence-free reconstruction of magnetic fields.

iii) Genuinely Multidimensional Riemann Solver.

iv) High Order Temporal Update. Use Runge-Kutta or use ADER at high order.

Let us address each of these very briefly in the next several transparencies and for the simplest case of second order accuracy.

We have made all higher order extensions. Results shown in next section.

This need for **higher order accuracy** is motivated by the fact that astrophysicists are beginning to face up to the presence of **turbulence**. Such problems have **strong shocks**; we must handle shocks.

Turbulence simulations always require the **lowest possible numerical dissipation and dispersion**. High order accuracy is the only known way of beating down dissipation and dispersion.

III.1) High order WENO Reconstruction on Unstructured Meshes

Central Stencil S_0 for target triangle T_0

(Useful for **smooth flow**; central stencil is most stable.)

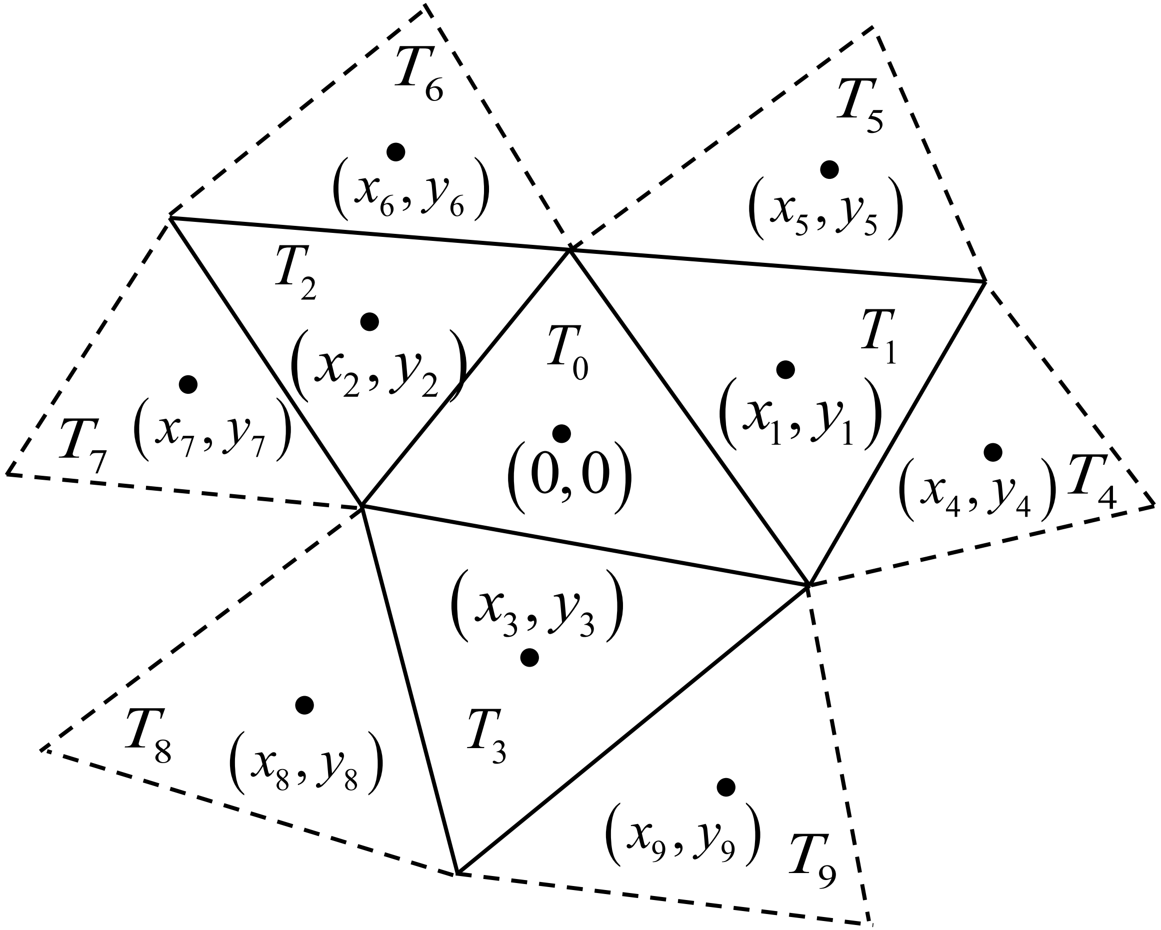

Each triangle starts with a single value for each variable.

Our Goal is to use neighbor information to obtain the slopes in the target triangle T_0 :-

$$u_{S0}(x,y) = \bar{u}_0 + \hat{u}_{S0;x} x + \hat{u}_{S0;y} y$$

Can be done by satisfying the over-determined system:-

$$\hat{u}_{S0;x} x_1 + \hat{u}_{S0;y} y_1 = \bar{u}_1 - \bar{u}_0 \quad ;$$
$$\hat{u}_{S0;x} x_2 + \hat{u}_{S0;y} y_2 = \bar{u}_2 - \bar{u}_0 \quad ;$$
$$\hat{u}_{S0;x} x_3 + \hat{u}_{S0;y} y_3 = \bar{u}_3 - \bar{u}_0 \quad ;$$

This is done in Least SQuares sense (LSQ).

One-Sided Stencils S_1 , S_2 & S_3 for target triangle T_0

(Useful at **shocks** are propagating from one or other side)

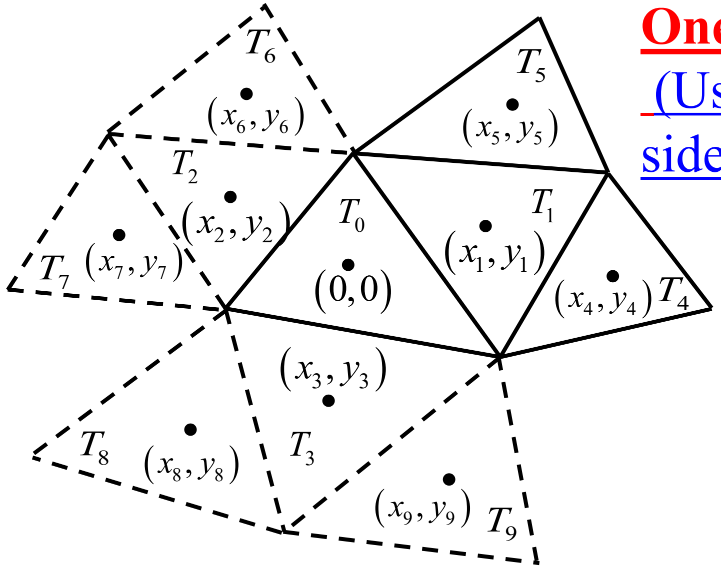

Upwind biased stencil S_1 ; Flow features upwinded towards left-lower corner of T_0.

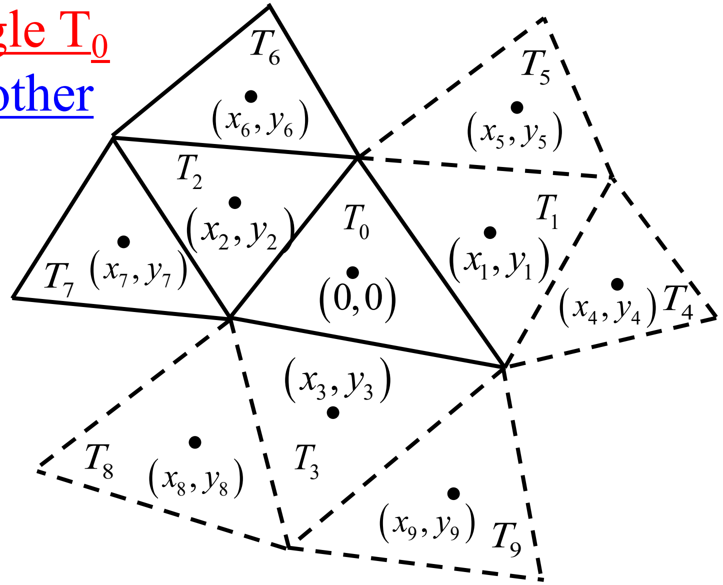

Upwind biased stencil S_2 ; Flow features upwinded towards right-lower corner of T_0.

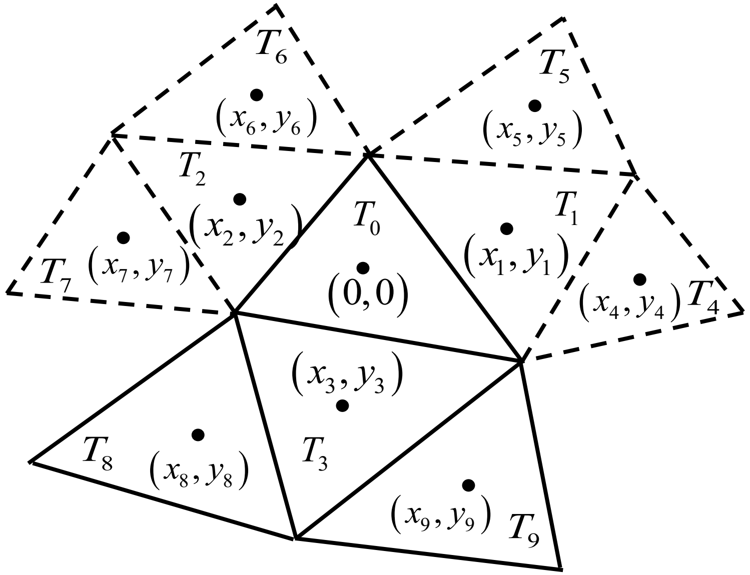

Upwind biased stencil S_3 ; Flow features upwinded towards upper corner of T_0.

The flow features can also be anisotropic, in which case a one-sided, upwind-biased stencil might be more appropriate. We show three possible one-sided stencils shown by the three sets of triangles $\{T_0, T_1, T_4, T_5\}$, $\{T_0, T_2, T_6, T_7\}$ and $\{T_0, T_3, T_8, T_9\}$. The stencils are shown by the solid lines. They correspond to flow features that might need to be upwinded towards one of the three vertices of triangle T_0 .

III.2) Divergence-free reconstruction of magnetic fields

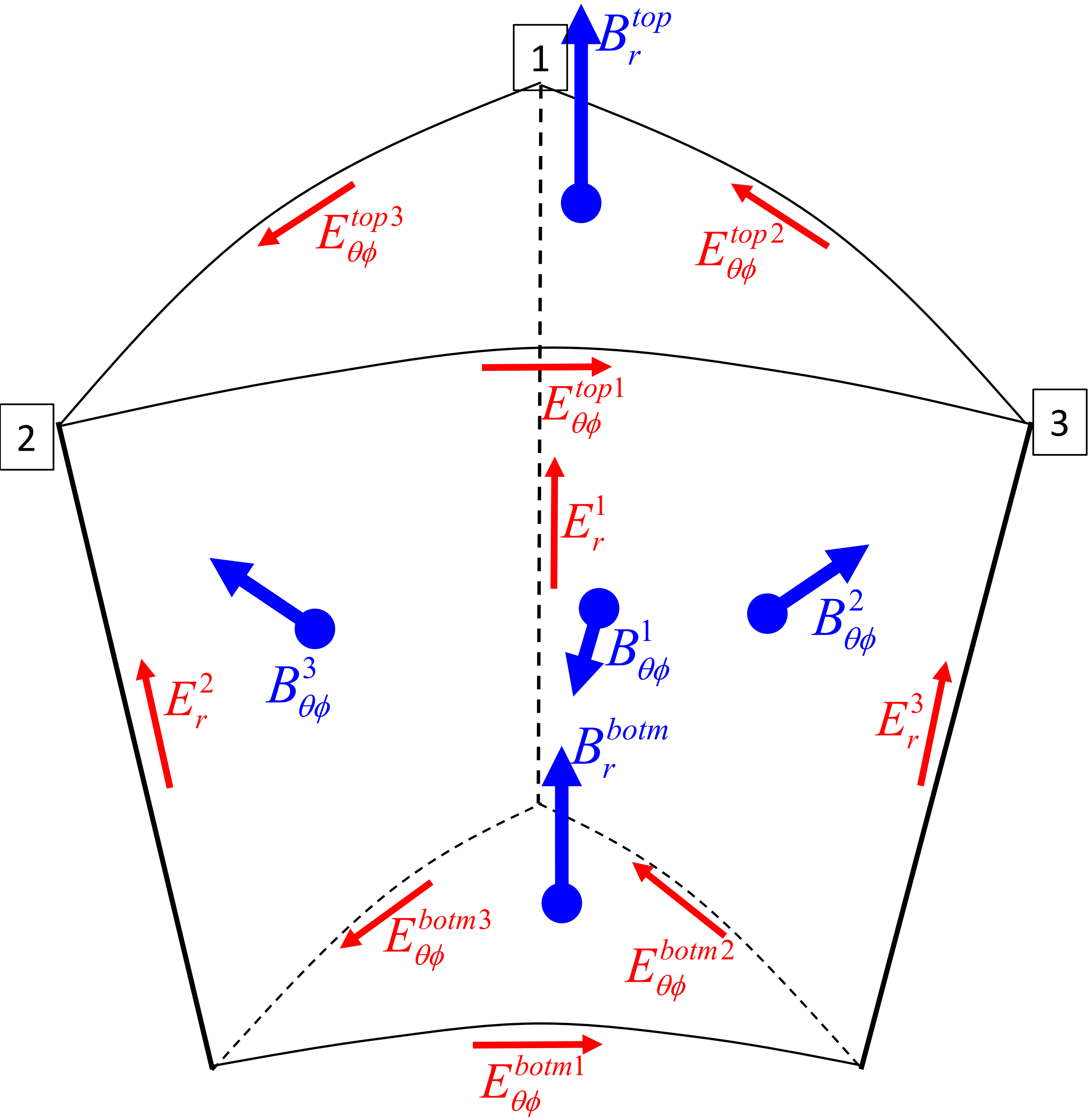

The elements form a 5-faced shape called a frustrum. Within each frustrum we make a zone-centered WENO reconstruction that is **not divergence - free**:-

$$B_x(x,y,z) = B_{x;0} + (\Delta_x B_x)x + (\Delta_y B_x)y + (\Delta_z B_x)z \quad ;$$
$$B_y(x,y,z) = B_{y;0} + (\Delta_x B_y)x + (\Delta_y B_y)y + (\Delta_z B_y)z \quad ;$$
$$B_z(x,y,z) = B_{z;0} + (\Delta_x B_z)x + (\Delta_y B_z)y + (\Delta_z B_z)z$$

Our Goal is to obtain a magnetic field reconstruction that is the closest possible to the one above, while also remaining **divergence - free**. We pick:-

$$B_x(x,y,z) = a_0 + a_x x + a_y y + a_z z + a_{xx}(x^2 - C_{xx}) + a_{xy}(xy - C_{xy}) + a_{xz}(xz - C_{xz})$$
$$B_y(x,y,z) = b_0 + b_x x + b_y y + b_z z + b_{yy}(y^2 - C_{yy}) + b_{xy}(xy - C_{xy}) + b_{xz}(xz - C_{xz})$$
$$B_z(x,y,z) = c_0 + c_x x + c_y y + c_z z + c_{zz}(z^2 - C_{zz}) + c_{xz}(xz - C_{xz}) + c_{yz}(yz - C_{yz})$$

III.3) Genuinely Multidimensional Riemann Solver

We want to accurately preserve the analogy between the CT update on rectangular meshes with the update on frustrums!

This Goal is exactly provided to us by the Multidimensional Riemann Solver.

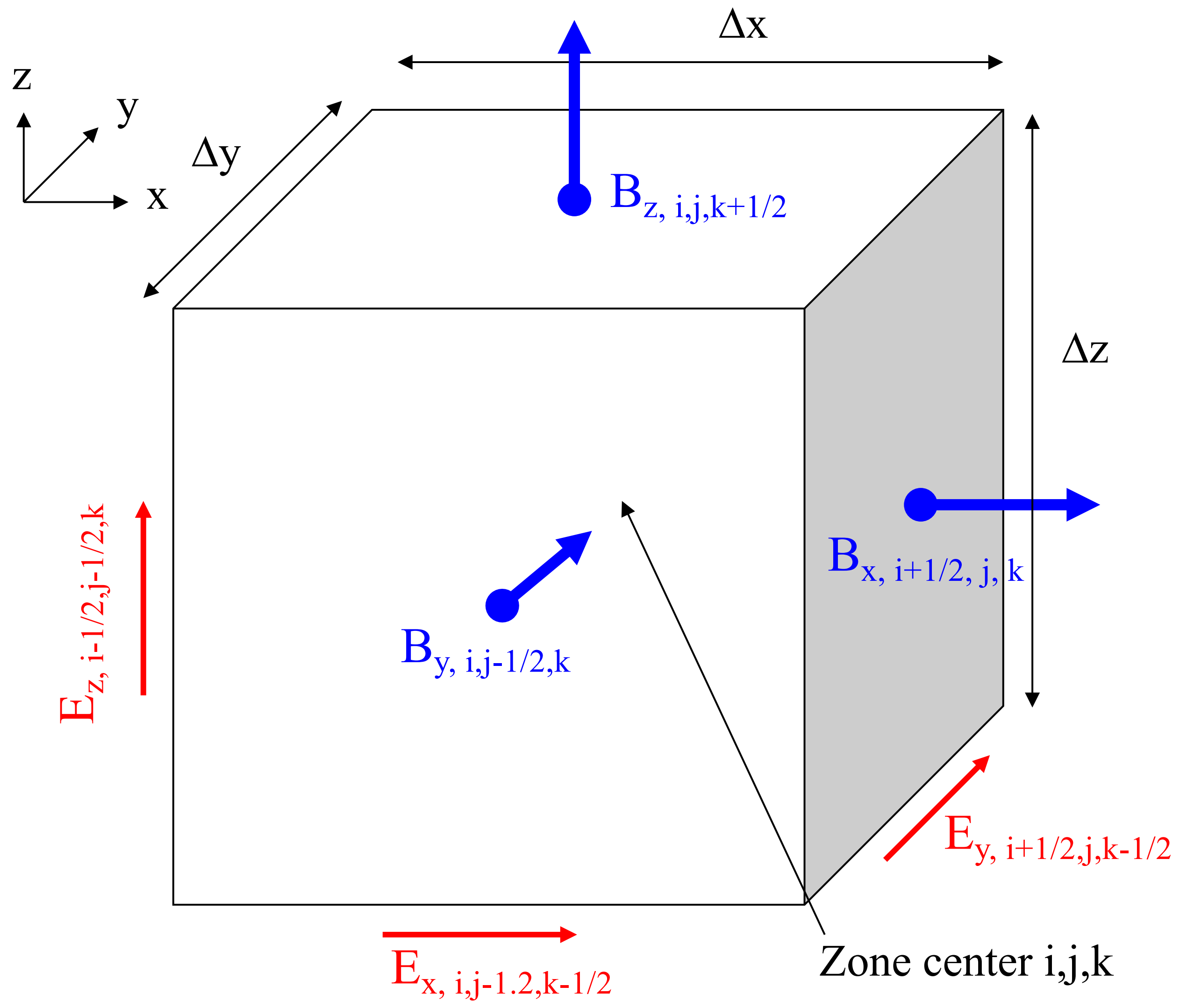

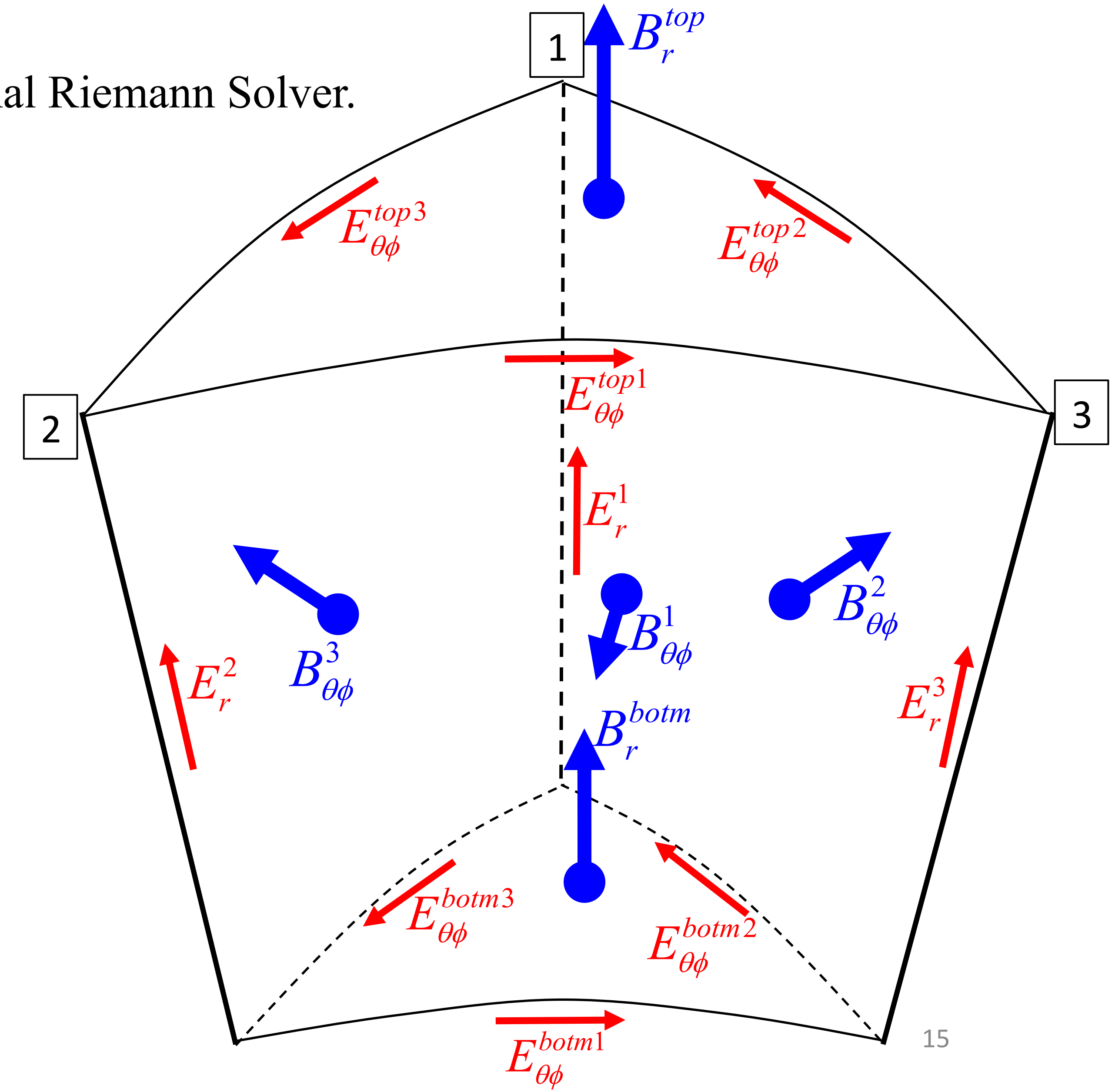

Test problem: stellar wind/inflow

Suggested by Ivan et al. (2015): interaction between two supersonic flows (point source plus uniform flow). A conservative solution is not known, so one is constructed (“manufactured”) by adding source terms to the MHD equations. The resulting flow has $\nabla\times\mathbf{u}=0$ and $\mathbf{u} \parallel \mathbf{B}$ everywhere.

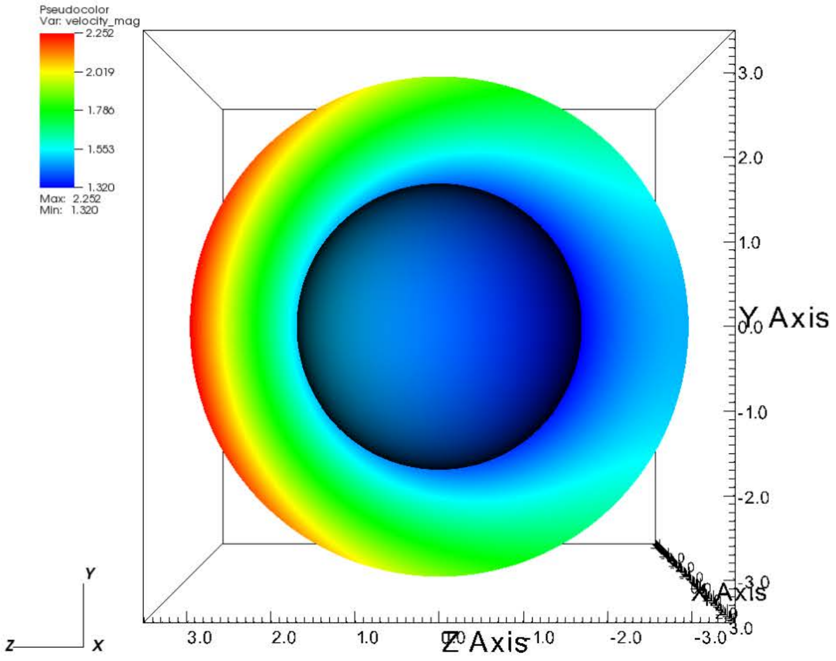

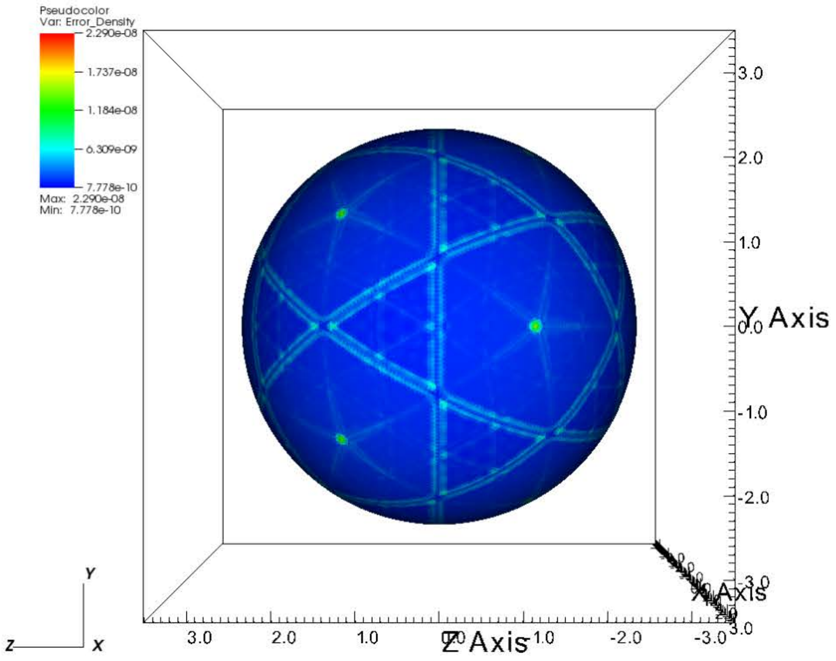

Results confirm 2nd, 3rd, and 4th order spatial accuracy. Right view shows the regular pattern of mesh imprinting.

Results: MHD Outflow with Method of Manufactured Solution Wind

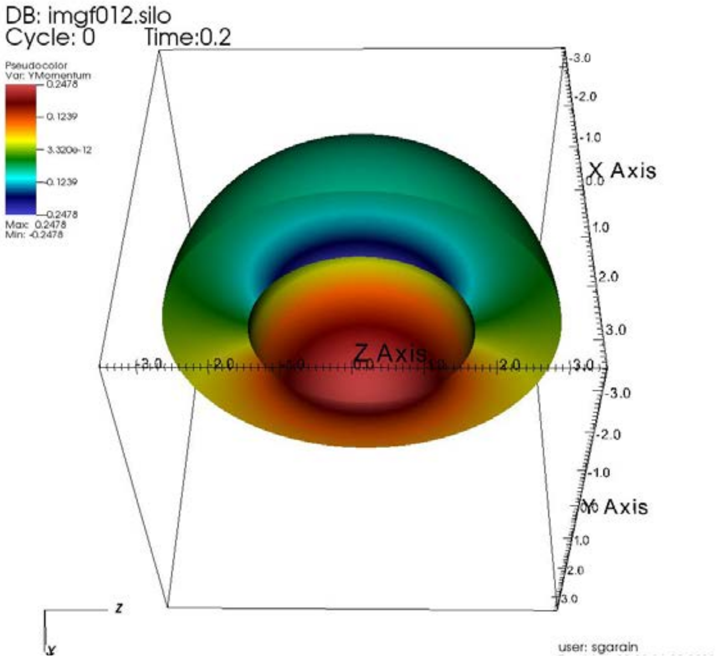

Y-Momentum

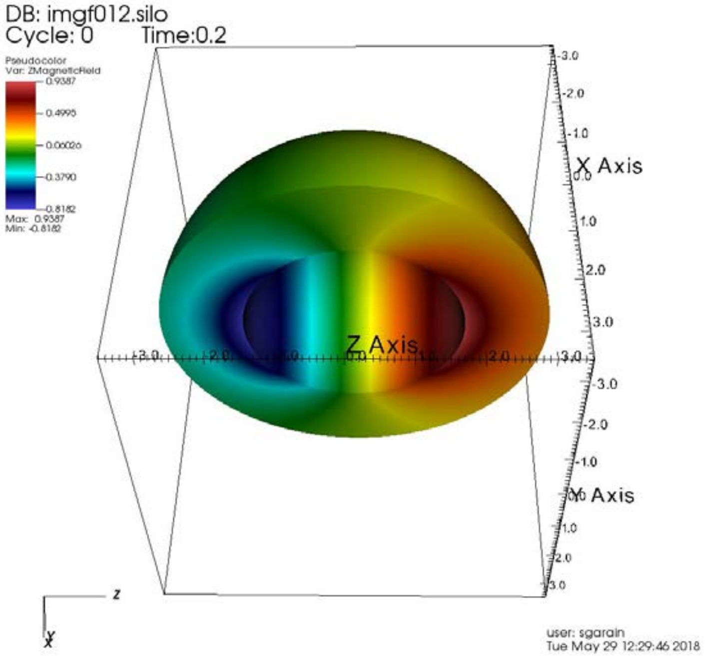

Z-Magnetic Field

Accuracy (x-Magnetic field)

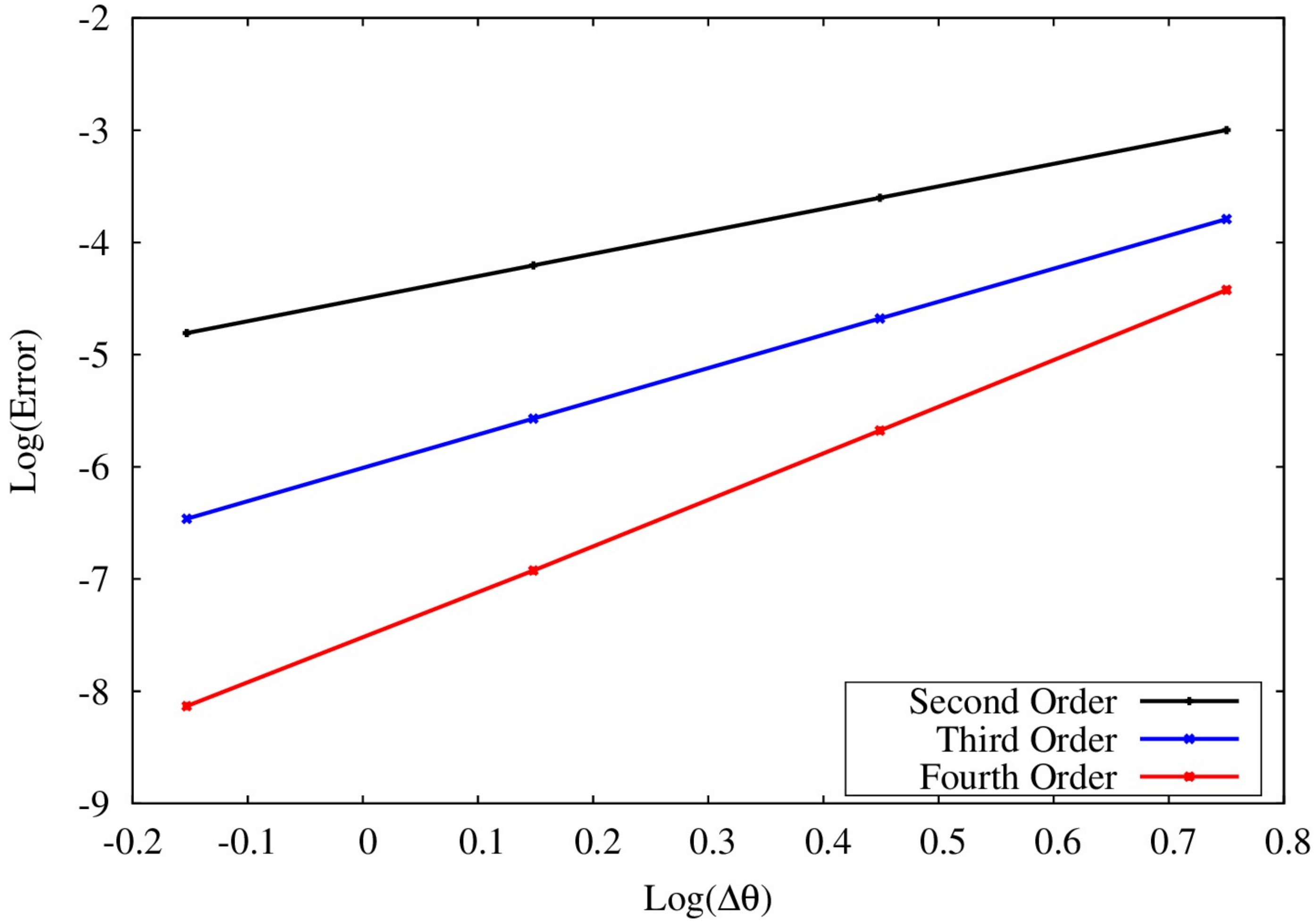

Δθ is measured in degrees.

Results: Exceptional Scalability of Geomesh MHD Code on Blue Waters

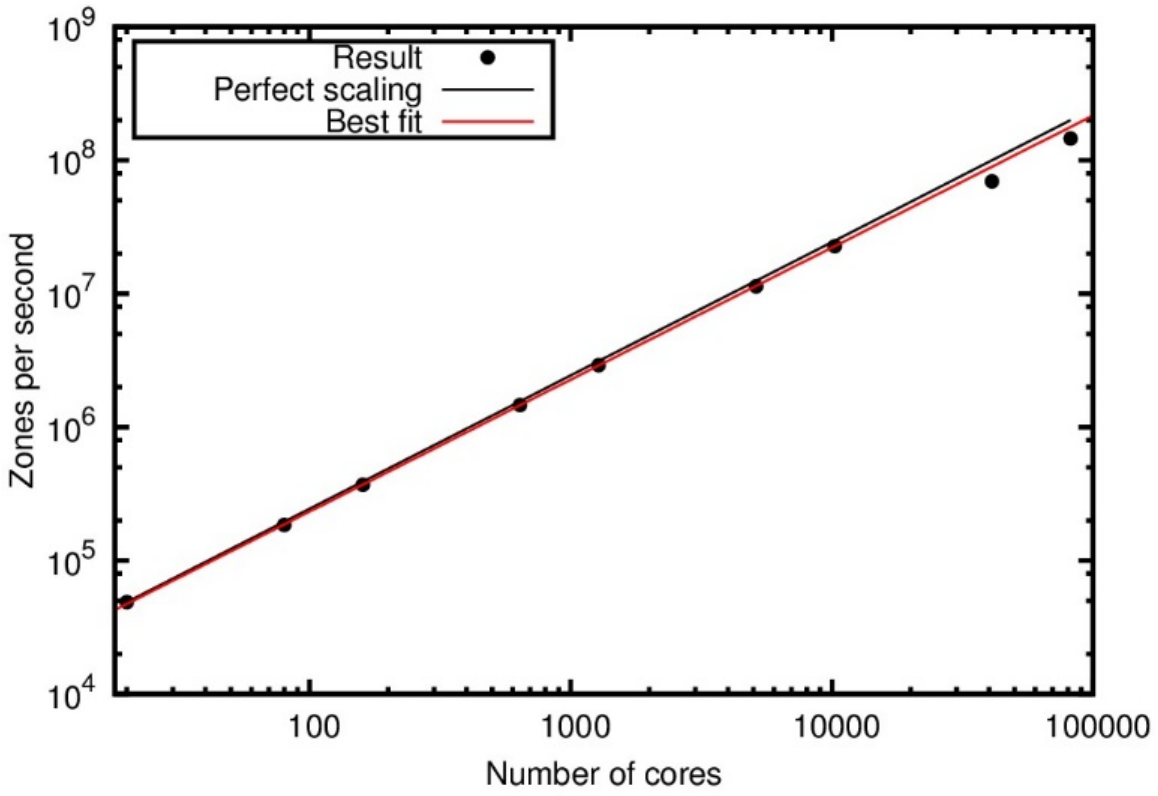

Second Order Scheme

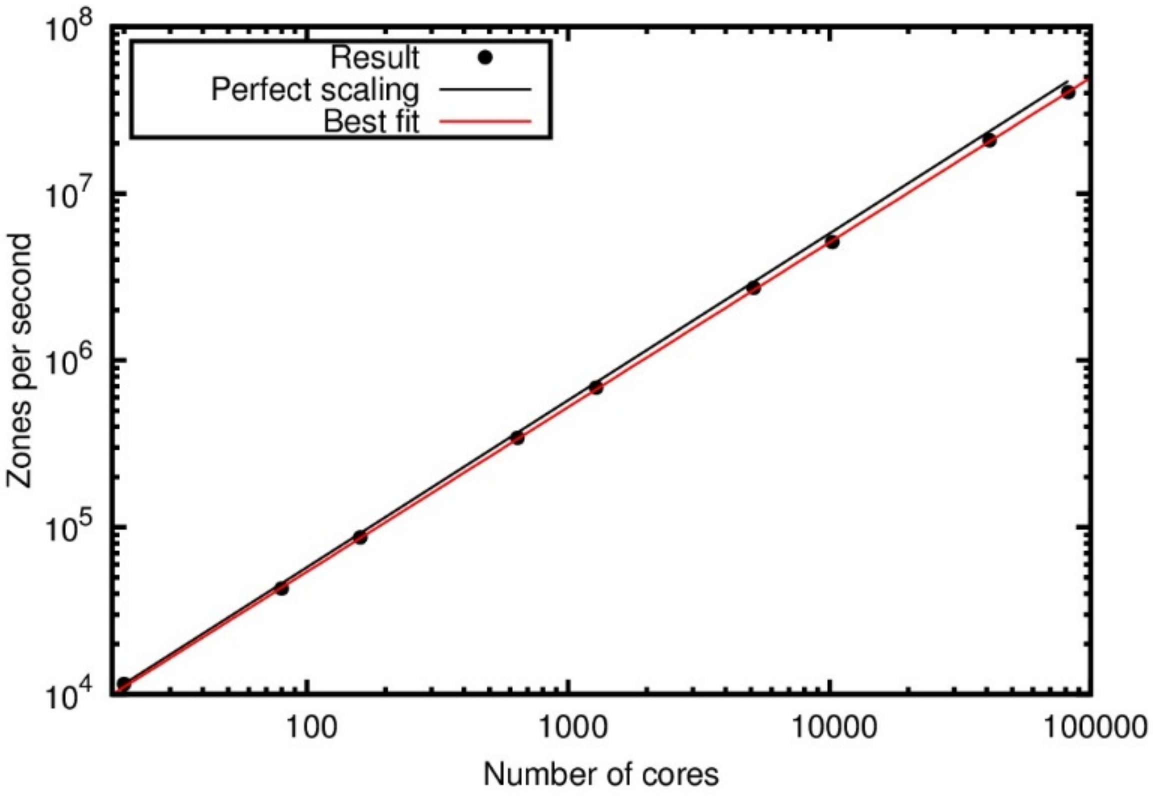

Third Order Scheme

Showing perfect scalability up to PetaScale on Blue Waters

Typical X-ray Observations from Black Hole Binaries

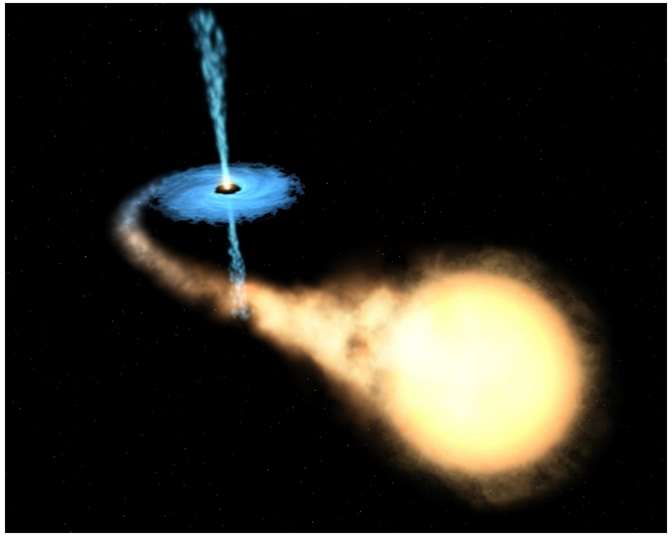

Light curve (top panel) and power density spectra (PDS; bottom panel) of GRO J1655-40.

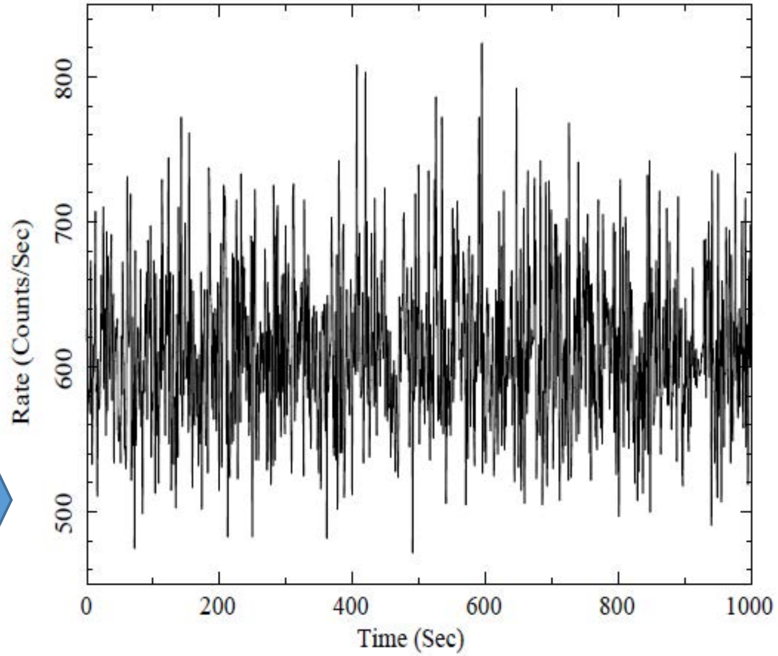

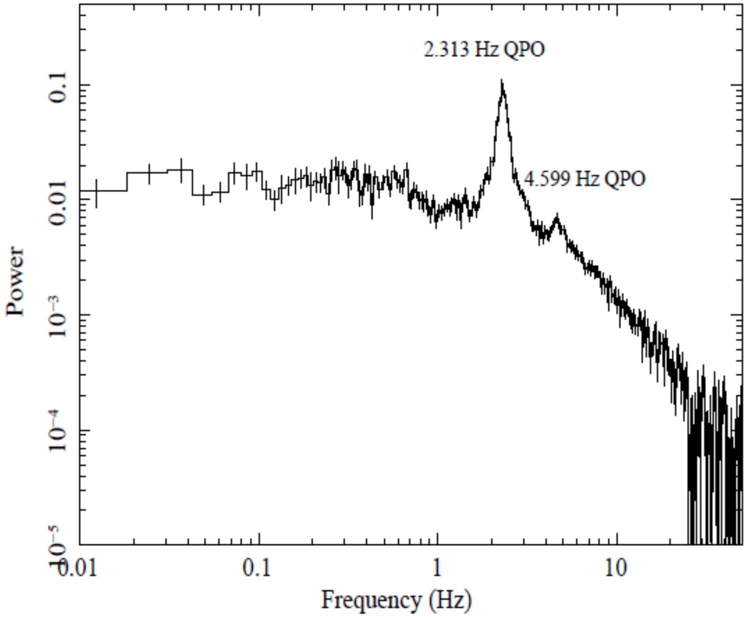

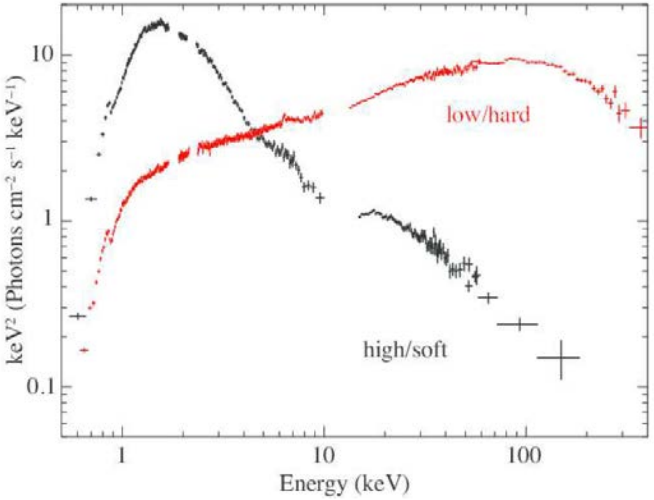

Suzaku spectra of black hole candidate Cygnus X-1. The black one was obtained in the high/soft state on 2010 December 16 and the red one was taken in the low/hard state on 2005 October 5.

IV) Results from Geodesic Mesh: Sub-Keplerian Accretion onto non-rotating black hole

Specific angular momentum λ = 1.5

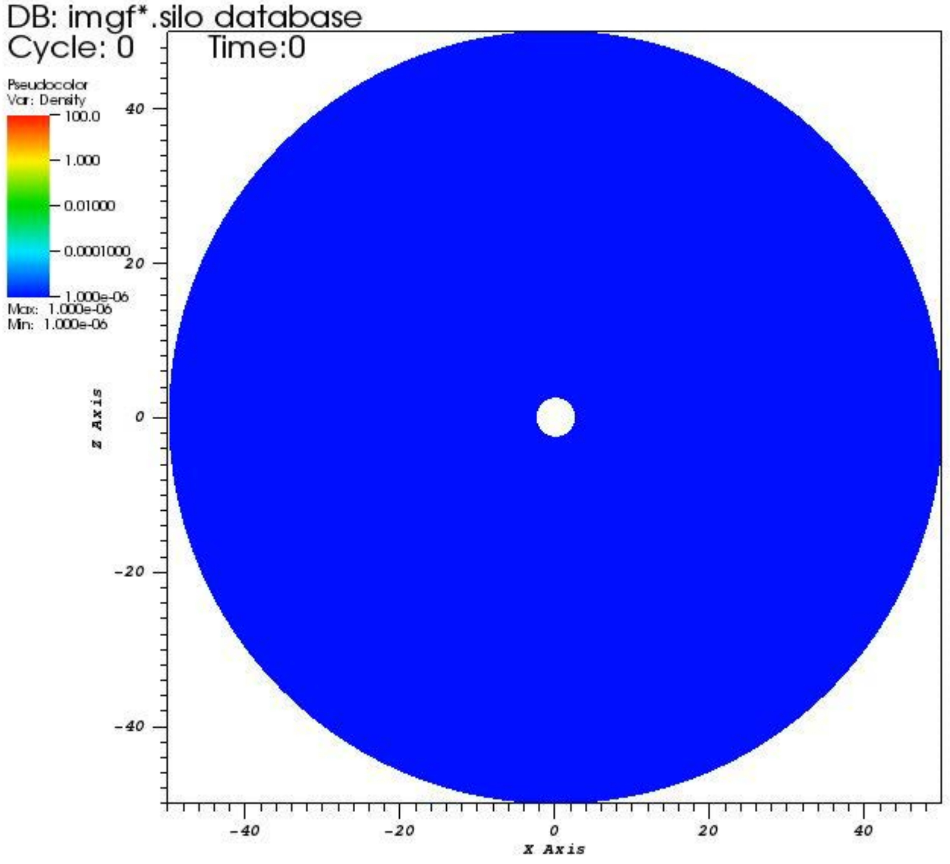

Meridional slice

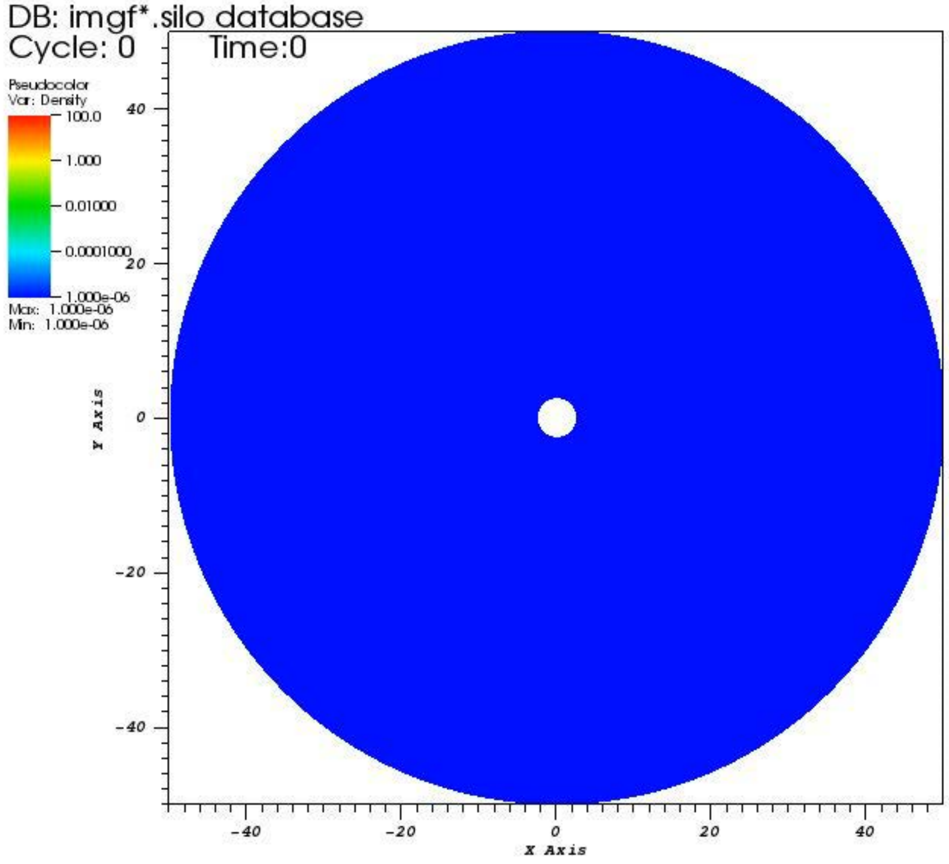

Equatorial slice

Simulation performed on a spherical geodesic mesh with angular resolution of 2.1^o and 200 logarithmically binned radial zones: r_{min} = 2.0 and r_{max} = 50.0

Results: Shock is on-average stable! Sub-Keplerian disk forms with oscillations that can explain the QPOs!

Stills:- Hydrodynamic Case

Density

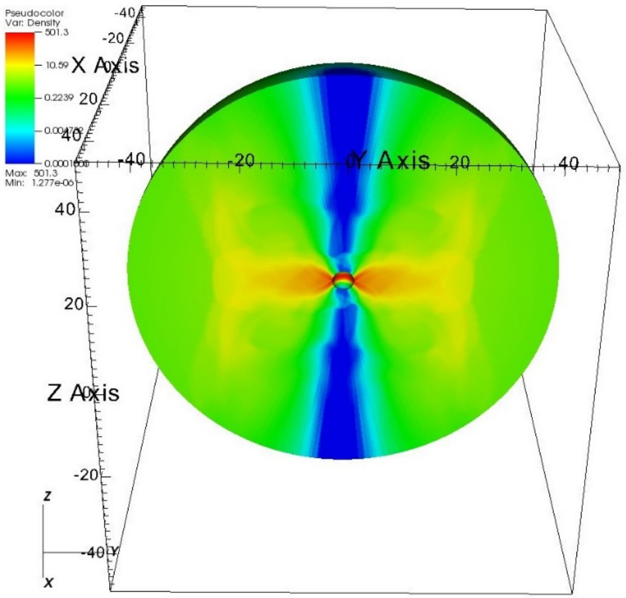

Pressure

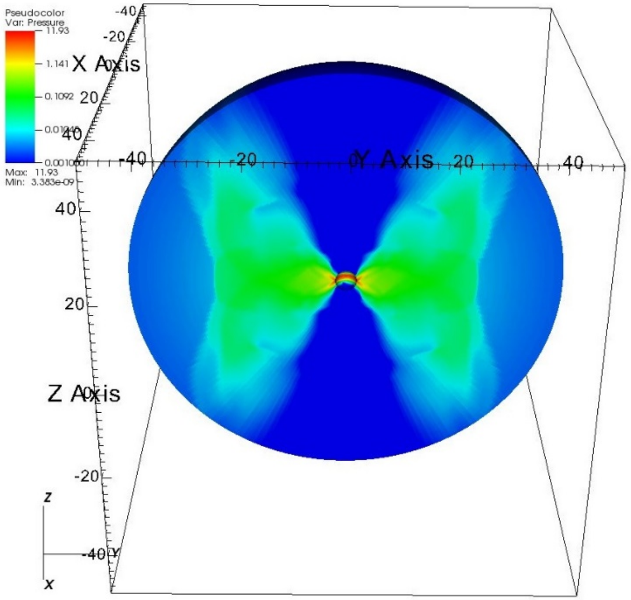

Density with Vel. Vectors Overlaid

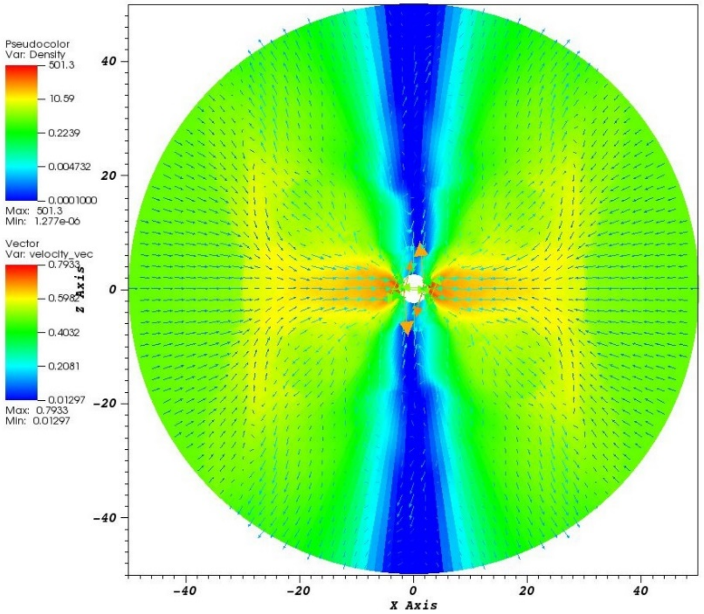

Advection of Field Loop: 3D simulation result

A toroidal field loop of plasma beta 10 is initialized inside the sub-Keplerian accretion flow

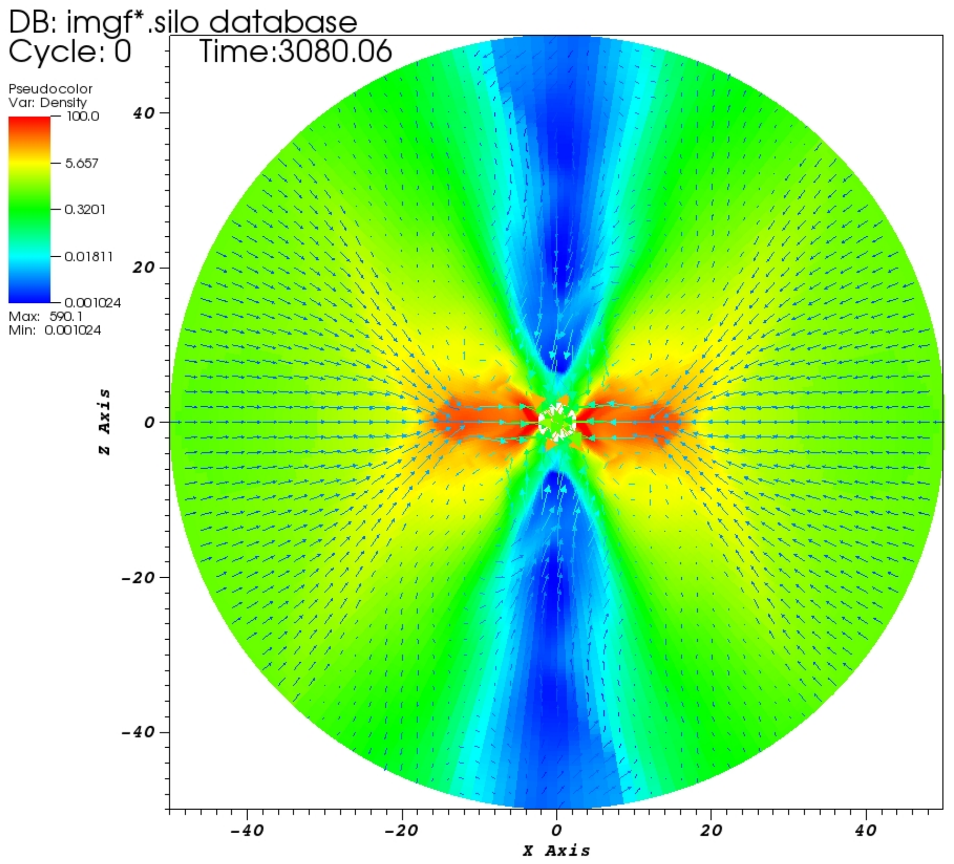

Initial hydrodynamic configuration of the disk

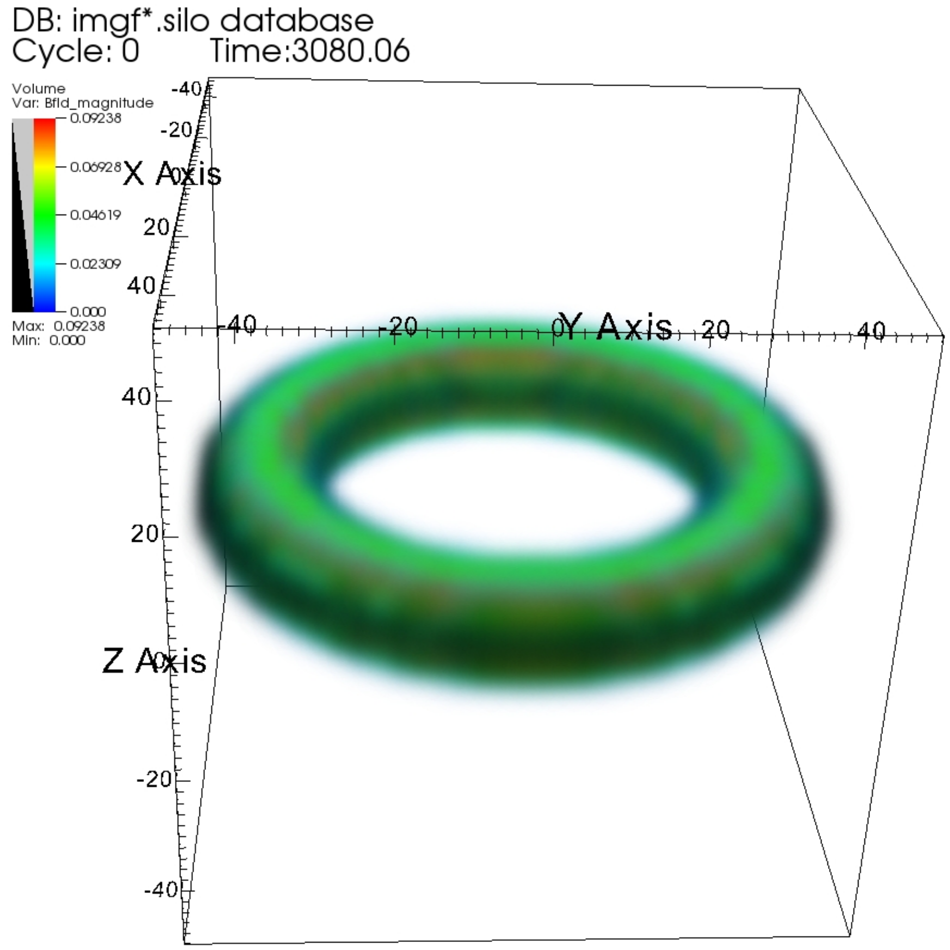

3-D visualization of the initial toroidal field loop

Accretion of Field Loop: 3D simulation result

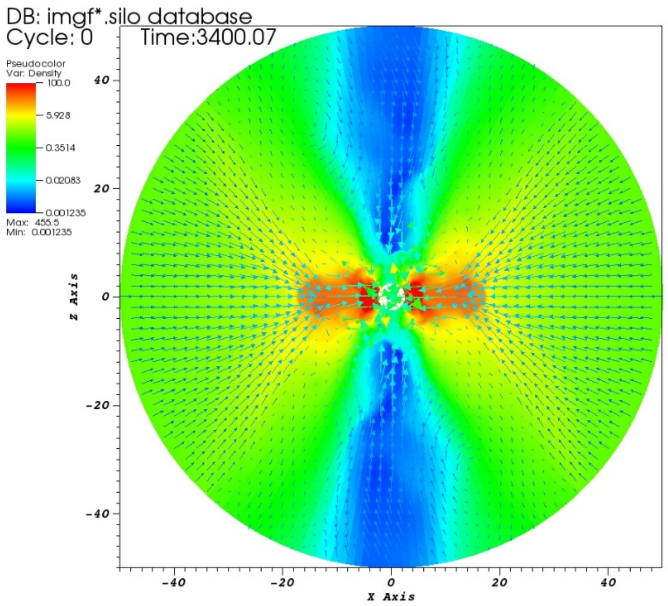

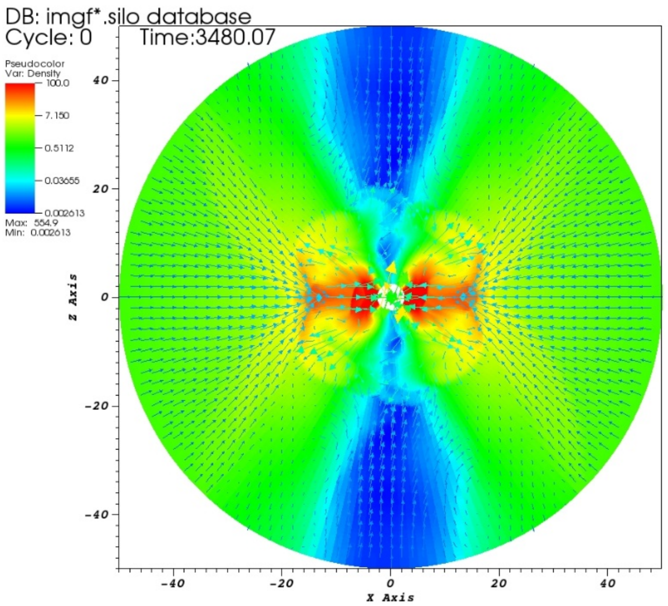

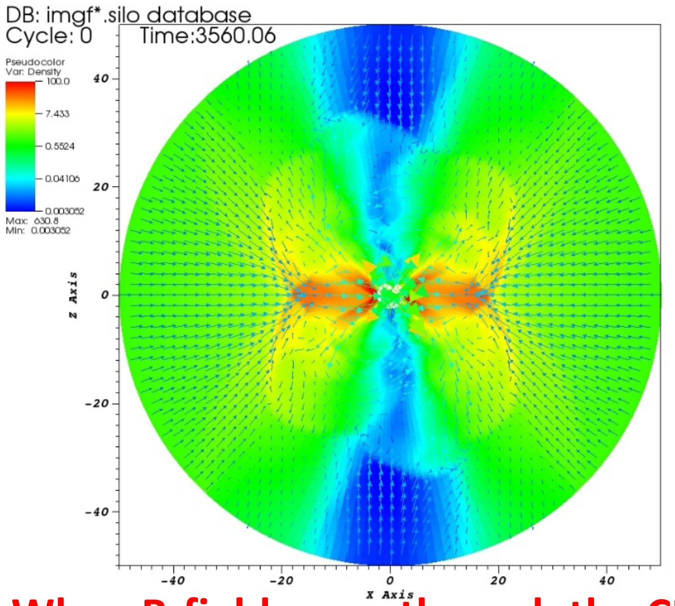

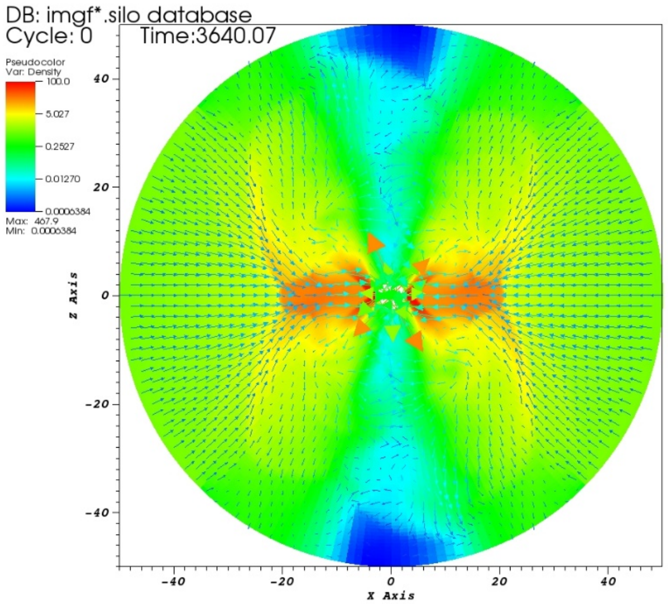

Results: When B-fields pass through the CENBOL shock, they launch jets! Jets are stable and fill up the funnel region. Any magnetic activity in CENBOL region will launch jets.

Stills: MHD Case

Density

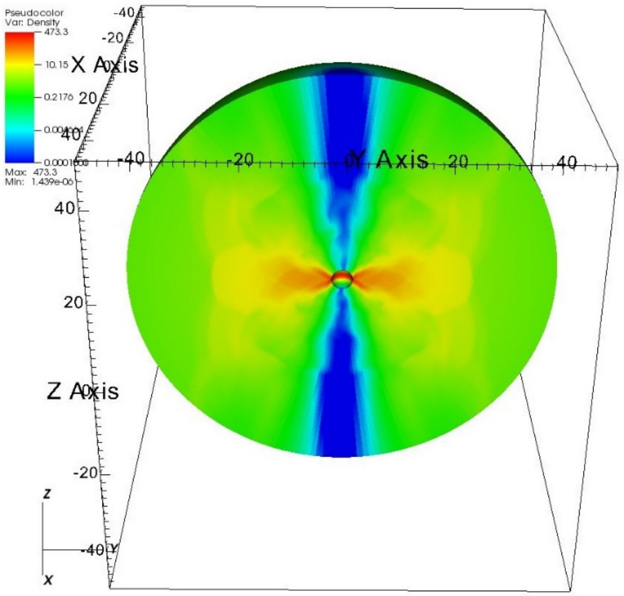

Pressure

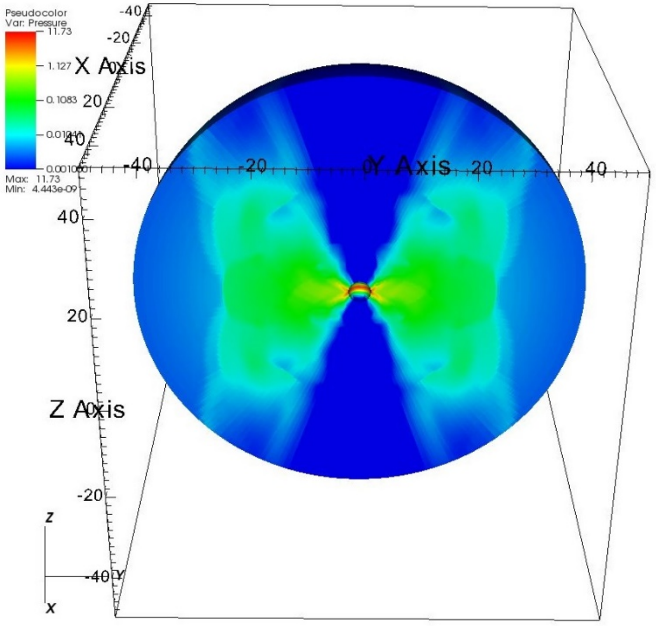

Density with
Vel. Vectors
Overlaid

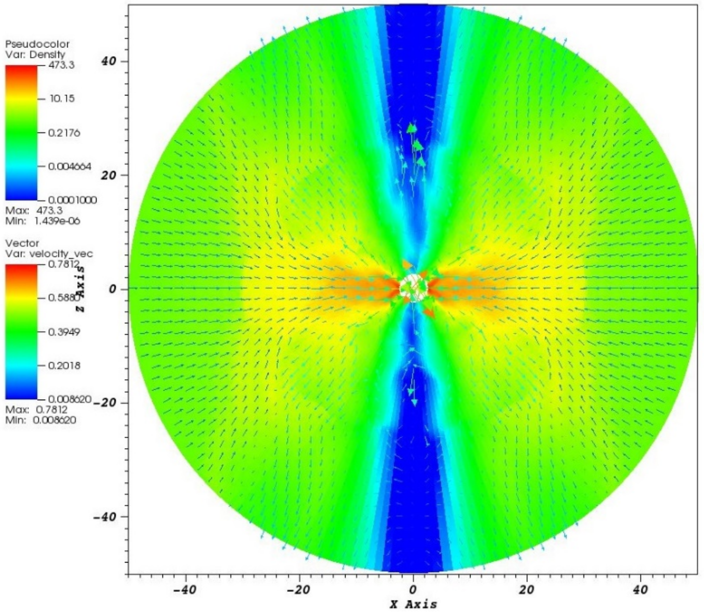

Magnetic
field
magnitude

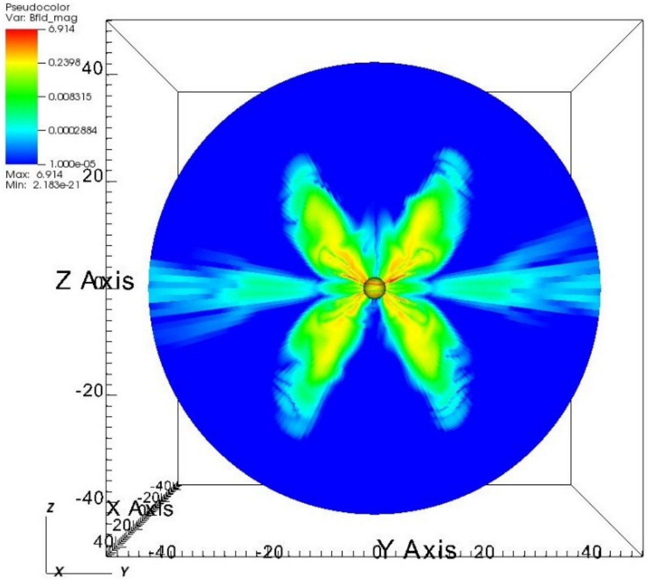

Results: Magnetic fields seem to want to reside on the funnel walls, even as jet accelerates in the funnel center.